# Quantitative estimation of electronic quality of zinc phthalocyanine thin films

Debdutta Ray,* Mauro Furno, Ellen Siebert-Henze, Karl Leo, and Moritz Riede
*Institut für Angewandte Photophysik, Technische Universität Dresden, 01062 Dresden, Germany*
(Received 6 April 2011; revised manuscript received 14 June 2011; published 15 August 2011)

We determine the mobility-lifetime product ($\mu\tau$) of free charge carriers in pristine zinc phthalocyanine (ZnPc) films using photocurrent measurements. The photocurrent is proportional to the free charge carrier generation efficiency ($\eta$) and the $\mu\tau$ product, and the carrier collection length is directly proportional to the latter. The $\mu\tau$ product is thus an important parameter for the electronic quality of a material. We further determine the dominant photocarrier generation mechanisms in ZnPc. The free carrier generation efficiency is estimated from total carrier collection and electric field–induced photoluminescence quenching measurements. Using $\eta$ and the electric field dependence of the photocurrent, we estimate the $\mu\tau$ product of holes in ZnPc to be about $3\times10^{-11}$ cm$^2$/V.

DOI: 10.1103/PhysRevB.84.075214 PACS number(s): 72.80.Le, 73.50.Pz, 88.40.jr, 78.55.Kz

## I. INTRODUCTION

Zinc phthalocyanine (ZnPc) is widely used as an absorber in organic solar cells.[1–4] ZnPc has a large absorption coefficient (peak value of $1.5\times10^5$ cm$^{-1}$) in the wavelength range of 600–750 nm and is hence a popular candidate for small molecular organic solar cells.[1–4] Bulk heterojunction solar cells composed of ZnPc (donor) and C60 (acceptor) have shown efficiencies greater than 2.5%.[3] One important parameter defining the power conversion efficiency of a solar cell is the fill factor, which is dependent on the carrier collection efficiency of a solar cell.[5] A material with large carrier collection efficiency is required for an efficient solar cell. The carrier collection length ($l$) defines the electronic quality of a sample and is given by the product of the carrier mobility ($\mu$), the carrier lifetime ($\tau$), and the electric field ($F$).[6–13] A clean material (i.e., a material with low impurity concentration or trapping centers) will have a large carrier collection length. Hence, it is important to evaluate the $\mu\tau$ product of the constituent materials of a solar cell to check their electronic quality. This will ultimately help in designing and fabricating better devices.

Photocurrent measurements can be used to determine the carrier collection length.[7,8,13] In many inorganic semiconductors, photons with energy greater than the bandgap of the semiconductor lead to the formation of free carriers at room temperature; hence, the free carrier generation efficiency ($\eta$) is nearly unity. Thus, in inorganic semiconductors, the measure of the photocurrent as a function of the electric field is a direct measure of the $\mu\tau$ product.[11,13] However, in most organic semiconductors, photoexcitations are excitonic with large exciton binding energies on the order of 0.5 eV.[14,15] Photocarrier generation may occur either spontaneously or with the assistance of an electric field in the bulk of the sample.[16–27] Additionally, photocarrier generation can also take place at an organic/metal or organic/organic interface.[28–32] To evaluate the $\mu\tau$ product, it is necessary to determine the photocarrier generation mechanisms and their efficiencies.

Although ZnPc has been intensively studied in donor-acceptor structures with C60 as the acceptor, its electronic properties in pristine form are less investigated.[33–37] In this work, we measure the photocurrent spectral response of pristine ZnPc as a function of applied reverse bias voltage to evaluate its carrier transport properties. The shape of the spectral response of the photocurrent is analyzed using optical simulations to determine whether photocarrier generation occurs dominantly at an interface or in the bulk of the sample. The carrier generation efficiency is measured from total carrier collection measurements and electric field–induced photoluminescence (PL) quenching. The $\mu\tau$ product has been measured for different thicknesses of the sample, with sample thickness varying from 50 to 200 nm. The $\mu\tau$ product has been found to be independent of the sample thickness. This procedure can be used to quantify the relative electronic quality of different batches and sources of the material quickly.

## II. EXPERIMENT

The devices are fabricated by depositing ZnPc (TCI Europe) under high vacuum conditions (base pressure $<10^{-8}$ mbar) on patterned indium tin oxide (ITO; Thin Film Devices)–coated glass substrates in a custom-made deposition system (K. J. Lesker, Hastings, UK). The system allows one to grow 16 samples in one run, thereby allowing similar deposition conditions for all the devices. A 100-nm-thick Al electrode is grown on top of the material and it formed the top electrode. Typical device geometry is ITO/ZnPc ($L$ nm)/Al (100 nm), where $L$ is the thickness of the ZnPc film and varies from 50 to 300 nm. All devices have an active layer area of 6.4 mm$^2$. In some devices, a thin layer of C60 (BuckyUSA) is deposited between the ZnPc and Al contact to enhance photocarrier generation at this interface. The thickness of the C60 is either 5 or 10 nm. Thicknesses of the samples are measured using a quartz crystal microbalance during growth. Nominal thicknesses are checked by measuring the capacitance of the devices. Because the devices are undoped, capacitance is equal to the geometric capacitance and is independent of voltage in reverse bias.[7,38] ZnPc and C60 have been purified at least twice using train sublimation. After deposition, the devices are encapsulated with glass in a nitrogen glovebox attached to the deposition system. Therefore, the devices are never exposed to air. All measurements are made at room temperature.

The modulated photocurrent is measured with a lock-in amplifier (Signal Recovery SR7265) phase set to the frequency of the mechanical chopper used to chop the incident light. The advantage of measuring the modulated photocurrent is that the dark current is subtracted automatically; hence, it is possible to measure the photocurrent with very high precision.

 

The monochromatic light used for excitation is incident on the sample through the transparent glass/ITO interface. Hence, ITO formed the near electrode, and Al the far electrode. The light source is a Xe lamp coupled with a monochromator (Newport Oriel Apex). The intensity of the incident light is measured at each wavelength with a calibrated Si photodiode (Hamamatsu). The spectral response of the photocurrent is measured at different bias voltages applied to the device.

PL quenching as a function of electric field is measured by applying a modulated voltage, with the use of a signal generator (HP 8114A), on the device while exciting the device at 633 nm using a HeNe laser (output power 0.6 mW). The device is excited through the transparent glass/ITO electrode, and the PL is detected through the same electrode. The change in PL ($\Delta$PL) with electric field is measured with a lock-in amplifier (Stanford Research Systems SR830) phase set with the modulation of the applied bias. $\Delta$PL is equal to PL(0)−PL($F$), where PL(0) is the PL at zero-applied electric field and PL($F$) at electric field $F$. The amplitude of the voltage modulation is varied to estimate the variation of $\Delta$PL with electric field. PL(0) is measured by chopping the incident light with a mechanical chopper and measuring the PL with a lock-in amplifier phase set with the chopping frequency. The onset of PL in ZnPc is at around 800 nm, and a 715 nm long-pass optical filter is used to cut off the scattered laser beam.[33] The total signal from the scattered laser light and any PL emanating from the color filter is 50 times smaller than the PL signal from the device. Hence, the error in estimating PL(0) is negligible (less than 2%). Care is taken that the illumination area is smaller than the device area so that PL(0) is not overestimated. The field-induced PL quenching measurements are done in reverse bias (negative voltage applied to the ITO electrode) so that there is no electroluminescence from the devices. Note that the detector picks up the total PL signal because we use a long-pass filter.

## III. RESULTS AND DISCUSSION

Figure 1 shows the spectral response of the photocurrent for a 200-nm-thick ZnPc sample measured at different voltages in reverse-biased conditions. Reverse bias is defined as negative bias applied to the ITO electrode. Under reverse bias, holes are collected at the ITO electrode and electrons at the Al electrode. Figure 1 also shows the absorption coefficient of ZnPc. As seen from the figure, the photocurrent spectral response does not follow the absorption coefficient. There can be two possible reasons for this observation. One of the reasons could be that the photocarriers are being generated dominantly by exciton dissociation at the far Al electrode.[7,28] Because ZnPc has a higher hole mobility compared with electrons, the photocurrent will be dominated by the hole component.[7,36,37,39] If the photocurrent is due to carrier generation at the far electrode, then it is possible that the photocurrent spectral response is antibatic with the absorption.[7,27,28] In such a case, the photocurrent will have maxima at the absorption edge and minima at the absorption maxima.[7,27,28] The photocurrent, when photocarrier generation takes place dominantly at the far electrode, can be written as[28]

$$J_{PC,\mathrm{far}} = \frac{\alpha\varphi\eta_i e}{(1/L_D)-\alpha}\exp(-\alpha L), \qquad (1)$$

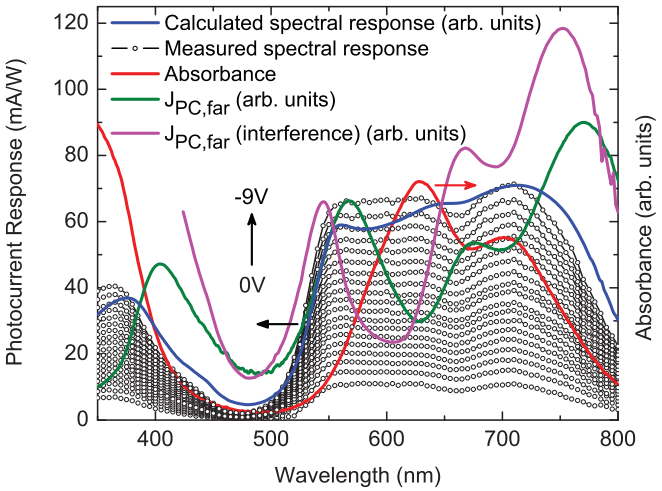


FIG. 1. (Color online) Photocurrent spectral responses measured at various reverse bias (from 0 to −9 V) are plotted for an ITO/ZnPc (200 nm)/Al device. The absorption coefficient of ZnPc, the photocurrent spectral response calculated from optical simulations taking into account bulk photon absorption as described in the text, and the spectral response of $J_{PC,\mathrm{far}}$ (both with and without optical interference effect) are also plotted for comparison.

where $\alpha$ is the absorption coefficient for the excitation wavelength, $L$ is the length of the sample, $e$ is the electronic charge, $L_D$ is the exciton diffusion length, $\varphi$ is the incident photon flux density and $\eta_i$ is the efficiency of exciton dissociation at the far interface. The spectral response of $J_{PC,\mathrm{far}}$ (normalized to be at the same scale as the photocurrent spectral response) is calculated for an exciton diffusion length of 10 nm and plotted in Fig. 1.[40,41] One can see that the experimental photocurrent spectral response and the calculated spectral response of $J_{PC,\mathrm{far}}$ do not follow each other. The optical density (OD) at 630 nm of a film 200 nm thick is around 1.3.[2] If the assumption of photocarrier generation at the far electrode was correct, then there should have been a photocurrent minimum at 630 nm. However, this is not observed. Thus, we can discount the fact that the far electrode acts as the center for photocarrier generation, which dominates the photocurrent. Later in this paper, we will show further proof of this.

The second reason the photocurrent does not follow the absorption coefficient could stem from the important role optical interference plays in determining the shape of the photocurrent spectra.[42–44] To check this possibility, the spectral response is simulated by calculating the photon flux absorbed in the bulk of the material at each wavelength. The calculations are carried out by evaluation of the component of the Poynting vector in the direction perpendicular to the device surface by means of a transfer matrix approach.[42,44,45] The optical constants of the materials (real and imaginary part of the refractive index), used by the calculation algorithm, have been estimated from absorption and reflection measurements.[2] It should be noted that this calculation is purely optical and the calculation of the photocurrent spectral response assumes constant photocarrier generation efficiency over the whole spectral range. The photocurrent response calculated from the absorbed photon flux and normalized to be at the same scale

as the experimental photocurrent spectral response is plotted in Fig. 1. It is seen that it follows similar trends as that of the measured photocurrent spectral response. The effect of optical interference is also applied for photocarrier generation at the far interface. The photon flux absorbed within one exciton diffusion length from the far interface is calculated. The corresponding photocurrent spectral response, for the case when these excitons diffuse and dissociate at the far electrode, is plotted in Fig. 1. As seen from the figure, the spectral response of $J_{PC,\mathrm{far}}$, both with and without an optical interference effect, shows similar trends and is very different from the measured data.

To check that photocarrier generation occurs dominantly in the bulk of the sample and optical interference plays the major role in determining the shape of the photocurrent response, the above analysis is carried out for films with different thicknesses. Figure 2 shows the photocurrent spectral response of films with thicknesses ranging from 50 to 300 nm. The calculated photocurrent spectral response is also plotted for comparison. It is seen that the calculated and the actual spectral response of the photocurrent follows each other reasonably well. This proves that photocarrier generation takes place in the bulk of the sample and is further proof that photocarrier generation efficiency is independent of the energy of incident photons; hence, we can discount preferential photocarrier generation from the so called B-band (maximum at 340 nm and claimed to be related to a mixed order of aggregates) or the Q-band (maxima at 633 and 699 nm and claimed to be related to dimers and higher order aggregates for the former and monomers for the latter) in ZnPc.[33,46–48]

As a further proof that the photocurrent is dominated by carrier generation in the bulk, we intentionally enhance exciton dissociation at the far Al electrode by adding a thin layer of C60 (5 or 10 nm) between ZnPc/Al. A thin layer of C60 ensures a negligible contribution to the photocurrent from C60. The photocurrent spectral response for films with ZnPc thicknesses 100, 150, and 200 nm are shown in Fig. 3. The calculated photocurrent spectral response when photons are dominantly absorbed in the bulk is shown for comparison. Although the photocurrent is large at the absorption edges, it can be accounted for by the enhanced absorption in the bulk of the sample. Thus, the contribution to the photocurrent from carriers generated at the far interface is small, compared with the bulk generation, and can be ignored. From the calculations, it is also found that the photon flux absorbed in the bulk of ZnPc is much larger than that absorbed in the thin C60 layer for the full wavelength range in this study. This verifies the assumption that the contribution of C60 to the total photocurrent is negligible. This experiment proves that the total photocurrent, even if there is photocarrier generation at the far interface, is still dominated by bulk photocarrier generation in ZnPc.

Now that it is proven that the photocurrent is dominantly due to photocarrier generation in the bulk of the sample, we discuss the voltage behavior of the same. Figure 4 shows the voltage dependence of the photocurrent response for a 200-nm-thick sample when illuminated through the ITO interface at 630 nm illumination wavelength. As seen from Fig. 4, the photocurrent changes linearly with voltage. The photocurrent response is

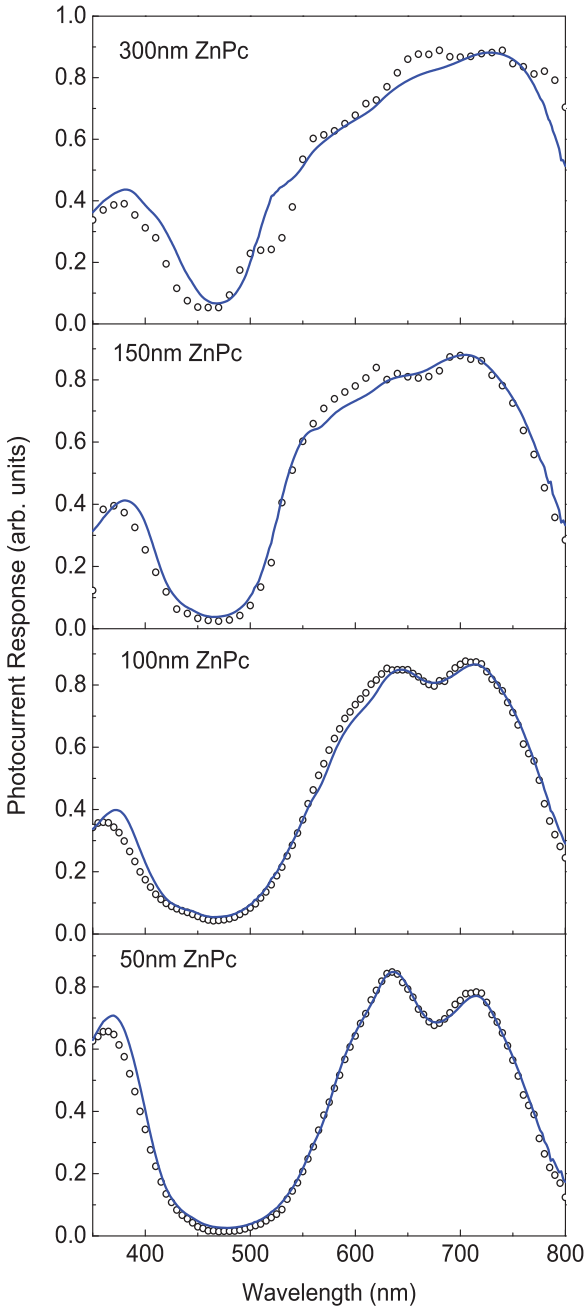


FIG. 2. (Color online) Photocurrent spectral response (open circles) measured in reverse bias for films with geometry ITO/ZnPc ($L$ nm)/Al, where $L$ varies from 50 to 300 nm, is plotted. The spectral response calculated from the optical simulations (line), which take into account bulk photon absorption, is plotted for comparison.

measured in reverse bias. The photocurrent ($J_{PC}$) for bulk carrier generation is given by[7,8,11,13,49,50]

$$J_{PC} = e\gamma\eta(l_p + l_n) = e\gamma\eta F(\mu_p\tau_p + \mu_n\tau_n), \qquad (2)$$

where $\eta$ is the free carrier generation efficiency, $\gamma$ is the rate of photons absorbed in the material per unit volume, $e$ is the electronic charge, and $l$ is the carrier collection length, and the subscripts $p/n$ define holes/electrons. The photocurrent, when photocarrier generation takes place in the bulk of the device, has been found to be dominated by the drift component, and

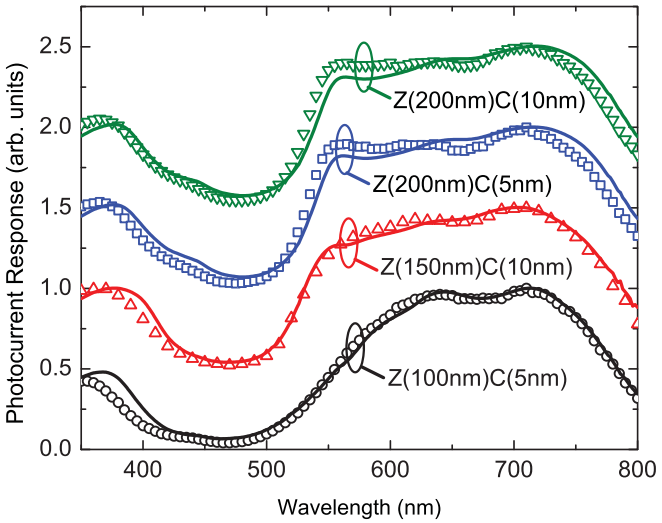


FIG. 3. (Color online) Photocurrent spectral response (open symbols) for devices with different layer thicknesses, in which a thin layer of C60 (5 or 10 nm) has been inserted between the far ZnPc/Al interface, is plotted. The plots for different films are displaced in the vertical axis for better visibility. The spectral response calculated from the optical simulations (line), which take into account bulk photon absorption, is plotted for comparison. The letters Z and C in the figure represent ZnPc and C60, respectively.

the diffusion component can be neglected.[7] In reverse bias, the maximum photocurrent gain is unity, and the electric field is uniform across the device.[7,38] It can be seen from Eq. (2) that PC is proportional to both the photocarrier generation efficiency ($\eta$) and the $\mu\tau$ product. The carrier collection length increases with increasing electric field as more carriers are collected. The carrier with the larger $\mu\tau$ product will dominate the carrier collection length and, therefore, the photocurrent. In the case of ZnPc, holes are expected because they have higher mobility.[36,37,39] At fields in which all carriers are collected, the photocurrent will be independent of the electric field, and the saturated photocurrent is given by[7,8,13,49]

$$J_{PC,\mathrm{sat}} = e\gamma\eta L \quad \text{for} \quad (l_p + l_n) \gg L. \tag{3}$$

In this analysis, we have assumed that the electric field dependence of the photocurrent is due only to the field term in the carrier collection length. However, there can be two more sources for the electric field dependence of the photocurrent. The first is from any field dependence of mobility.[51–53] The small bandwidths or the absence of bands in organic semiconductors means that carriers move by hopping along a manifold of discrete levels spread out both in energy and space.[51–53] This can lead to a field dependence of mobility and is generally described by the form $\exp(\beta F^{1/2})$.[51–53] $\beta$ is the parameter defining the electric field dependence of the mobility. For small $\beta$, the electric field dependence from the mobility term is much weaker than the linear field term from the carrier collection. The second source that can lead to a nonlinearity in the photocurrent is electric field–enhanced photocarrier generation.[16–22] It is possible that the excitons, which are generally the primary photoexcitation and are dipoles, may dissociate under the application of an electric field. The field-dependent exciton dissociation has been studied for many organic semiconductors.[16–22] The total carrier generation efficiency ($\eta$) is the sum of the spontaneous carrier generation efficiency [$\eta(0)$] and the field-induced exciton dissociation efficiency [$\eta_q(F)$].[7,8] Hence,

$$\eta = \eta(0) + \eta_q(F). \tag{4}$$

For small field dependence of the mobility and for photocarrier generation dominated by the spontaneous term $\eta(0)$, the photocurrent is expected to vary linearly with the applied voltage. The linear variation of the photocurrent, as seen in Fig. 4, points to the fact that the photocarrier generation is spontaneous in nature. Figure 5 shows the voltage dependence of the photocurrent response for films with thicknesses ranging from 100 to 200 nm. The figure shows the photocurrent response for films with and without the thin layer of C60 (5 or 10 nm) sandwiched between ZnPc and Al. The photocurrent response is linear with voltage for all the films, and the $\eta\mu\tau$ product calculated from the data varies between $3.5\times10^{-12}$ and $4.8\times10^{-12}$ cm$^2$/V. Reverse photocurrent saturation is not observed in any of the data, possibly because the $\mu\tau$ product is not high enough to reach the condition of total carrier collection. The possibility for total carrier collection increases with decreasing film thickness. Hence, we study the thinnest film in the assembly, which has a thickness of 50 nm. Figure 6 shows the photocurrent response of a 50-nm-thick film as a function of applied electric field when illuminated at 630 nm. The photocurrent is linear at low fields, increases as $F^{1.4}$ at medium fields, and saturates at large reverse bias. We now analyze the electric field dependence of the photocurrent in the three different field regimes.

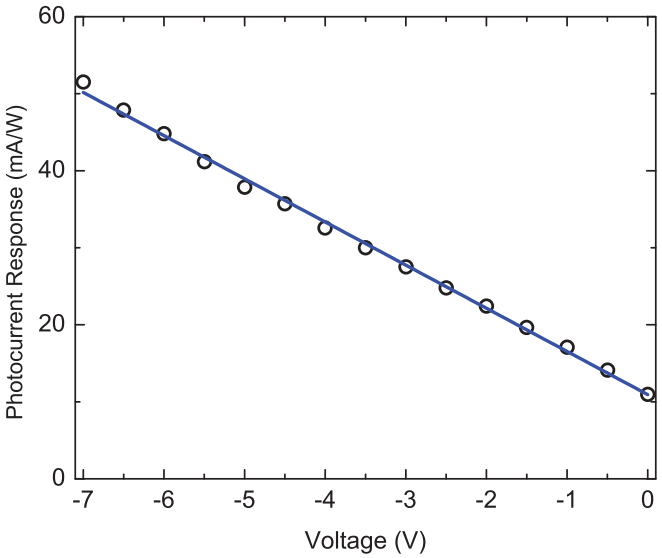


FIG. 4. (Color online) Photocurrent response (open circles) as a function of voltage is plotted for a ITO/ZnPc (200 nm)/Al device when illuminated at 630 nm. The photocurrent response is fitted with a linear function (line). The slope of the fit is proportional to the $\eta\mu\tau$ product.

In the low field regime ($F < 4.4\times10^5$ V/cm), as per the above analysis, the photocurrent is probably due to spontaneous photocarrier generation. At large electric fields ($F > 1.3\times10^6$ V/cm) the photocurrent saturates with electric

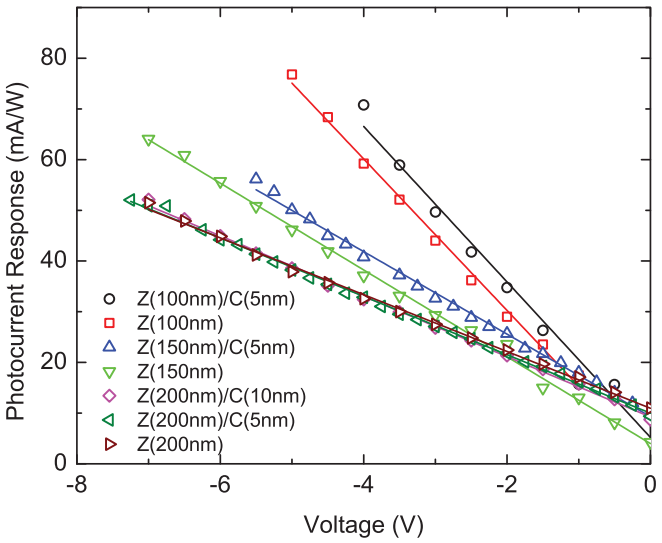


FIG. 5. (Color online) Photocurrent response (open symbols) as a function of voltage is plotted for films in the geometry ITO/ZnPc ($L$ nm)/C60($x$ nm)/Al when illuminated at 630 nm. The letters Z and C in the figure denote ZnPc and C60, respectively. The plots are fitted with a linear function of the voltage (line). The slope of the fit is proportional to the $\eta\mu\tau$ product.

field. Photocurrent saturation means that it is no longer a function of the carrier transport parameters ($\mu$ and $\tau$) and is given by Eq. (3). The only unknown parameter in Eq. (3) is $\eta$. $\gamma$ is calculated from the optical simulations referred to earlier, in which the incident intensity is found from the calibrated photodiode and described in the experimental section. Using these values, $\eta$ is found to be 0.5. The right-hand axis of Fig. 6 is scaled to $\eta$ using this calculation. This is quite a large value for the carrier generation efficiency. However, the nonlinearity of the photocurrent in the middle regime of the electric field

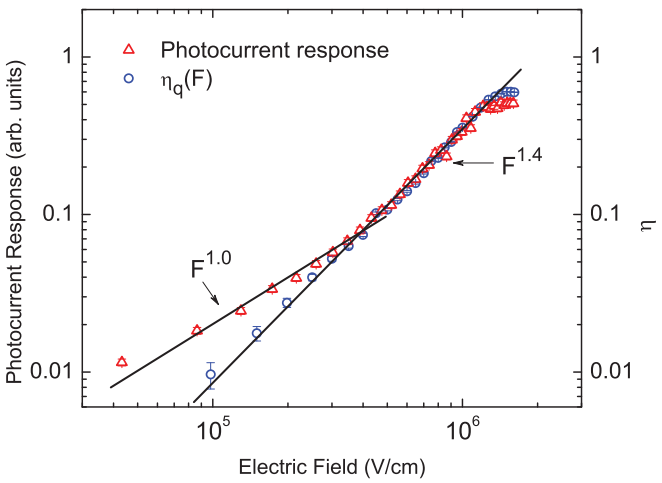


FIG. 6. (Color online) Photocurrent response (open triangles) and $\eta_q(F)$ (open circles) are plotted. The right-hand axis is scaled to $\eta$, as described in the text. The photocurrent is linear with electric field in the small field regime ($F < 4.4\times10^5$ V/cm), and increases as $F^{1.4}$ in the medium field regime before saturating at about $1.3\times10^6$ V/cm. The photocurrent follows $\eta_q(F)$ in the medium and high field region. Slopes of $F^{1.0}$ and $F^{1.4}$ are drawn for comparison.

($4.4\times10^5$ to $1.3\times10^6$ V/cm) suggests that the photocarrier generation efficiency is not only attributable to $\eta(0)$ in this region but may also be influenced by $\eta_q(F)$. To evaluate the field-induced photocarrier generation, we estimate the field-dependent photoluminescence quenching of the film.[7,8] PL(0) is defined as the photoluminescence at 0 field and PL($F$) is at field $F$; thus,[7,8]

$$\eta_q(F) = \frac{\mathrm{PL}(0) - \mathrm{PL}(F)}{\mathrm{PL}(0)}. \quad (5)$$

The $\eta_q(F)$ measured from photoluminescence quenching as a function of electric field is plotted in Fig. 6. It is seen that $\eta_q(F)$ is equal to $\eta$ in the medium and large electric field regime. At low fields, $\eta_q(F)$ decreases faster than the photocurrent. If the photocurrent were dominated by $\eta_q(F)$ in this region, then the photocurrent should have decreased at a faster rate (because it is a higher order function of the electric field) than $\eta_q(F)$ and not the other way around, as observed here. Thus, at small electric fields ($F < 4.4\times10^5$ V/cm), $\eta$ is dominated by $\eta(0)$, and at the transition from the low field to medium field regime, $\eta(0)$ and $\eta_q(F)$ become comparable. From this comparison, $\eta(0)$ is estimated to be around 0.11. Using this value, the $\mu\tau$ product for holes in ZnPc is estimated to be approximately $3\times10^{-11}$ cm$^2$/V. Because the photocurrent is given by only $\eta_q(F)$ in the medium field region, we can conclude that there is no contribution to the photocurrent from the transport terms in this region. Hence, total carrier collection occurs at electric fields in the transition from the low to medium field region (about $4\times10^5$ V/cm). The carrier collection length calculated from the $\mu\tau$ product at this field is larger than the thickness of the sample and follows the condition for Eq. (3) to be valid ($l_p + l_n > L$). This is an independent validation of the quality of the estimated $\mu\tau$ product. The $\mu\tau$ product is found to be relatively independent of the thickness of the sample. This is expected because the electronic properties in the bulk of the sample are not expected to change with increasing thickness when grown under similar conditions. Compared with other organic materials, the $\mu\tau$ product for holes in ZnPc is close to that reported for holes in *N*,*N*'-diphenyl-*N*,*N*'-bis(3-methylphenyl)-(1,1'-biphenyl)-4,4'-diamine (TPD) and more than three orders of magnitude larger than that of electrons in tris (8-hydroxyquinoline) aluminum ($Alq_3$).[7,8] The average $\mu\tau$ product for free charge carriers in a-Si:H p-i-n type solar cells have been reported to vary between $1.7\times10^{-9}$ and $9.5\times10^{-9}$ cm$^2$/V, depending on preparation conditions.[11]

We note that the spontaneous photocarrier generation efficiency, $\eta(0)$, is relatively large, with a value of about 11%. To determine the exact reason for this is beyond the scope of this paper. However, we present possible reasons for this observation in this section. Although the primary photoexcitation in organic semiconductors is excitonic, it has been proposed that the absorption coefficient can be broken up into two terms, $\alpha$(exciton) and $\alpha$(CT), where the former leads to the creation of tightly bound excitons and the latter leads to the creation of loosely bound electron-hole pairs.[24] If $\alpha$(CT) is small (less than 10% of the total absorption), it will not be observed in optical measurements and will only appear in measurements involving the creation of free charge carriers. It is possible that $\eta(0)$ is due to $\alpha$(CT). Relatively large

spontaneous photocarrier generation efficiency in organic semiconductors has been reported earlier.[8,23–25] $\alpha(\mathrm{CT})/\alpha$, measured by electroabsorption, has been reported to be 0.03 for anthracene.[24] Spontaneous photocarrier or polaron generation has been reported in conjugated polymers.[54–56] Miranda *et al*. has reported high quantum yield (10%) of spontaneous polaron generation in pristine conjugated polymer films where the generation efficiency is weakly dependent on the excitation energy.[54] It has to be noted that pristine ZnPc forms polycrystalline films where the degree of crystallinity is dependent on the substrate and the substrate temperature.[57] It is possible that excitons dissociate via defect states at the crystalline domain walls. Further studies are necessary to resolve this question.

To put things into perspective with respect to organic solar cells, the short-circuit current calculated from the photocurrent spectral response of the pristine ZnPc films is 0.2 $\mathrm{mA/cm^2}$. This is more than 20 times smaller than that observed in bulk heterojunction ZnPc/C60 films of similar geometry.[1–4] Thus, any contribution from the spontaneous photocarrier generation in ZnPc will not be observed in the solar cell geometry where photocarrier generation and possibly carrier collection is aided by C60. The higher mobility of electrons in C60 can be a reason for the latter.[58] The carrier recombination in solar cell geometries can also be the result of a different mechanism as the electrons and holes percolate along different material channels. This is another reason why it is necessary to study the materials in pristine form to evaluate the electronic properties of the individual materials.

## IV. CONCLUSIONS

The $\mu\tau$ product for holes in ZnPc has been estimated from photocurrent measurements and is found to be around $3\times10^{-11}$ $\mathrm{cm^2/V}$. The $\mu\tau$ product is a quantitative estimation of the electronic quality of a sample and is a very important parameter to evaluate materials from different batches or sources. It is seen that optical effects needs to be taken care of, particularly at wavelengths of low absorption, to understand the photocurrent spectral response. In pristine ZnPc films, photocarrier generation occurs dominantly in the bulk of the sample. From photocurrent and field-induced PL quenching measurements, the contributions of spontaneous and electric field–enhanced photocarrier generation has been separated.

## ACKNOWLEGMENT

The research leading to these results has received funding from the European Community's Seventh Framework Programme (FP7/2007-2013) under grant agreement No. 212311 of the ONE-P project.

*Corresponding author: debdutta.ray@iapp.de

[1] J. Drechsel, B. Männig, F. Kozlowski, M. Pfeiffer, K. Leo, and H. Hoppe, Appl. Phys. Lett. **86**, 244102 (2005).
[2] B. Maennig, J. Drechsel, D. Gebeyehu, P. Simon, F. Kozlowski, A. Werner, F. Li, S. Grundmann, S. Sonntag, M. Koch, K. Leo, M. Pfeiffer, H. Hoppe, D. Meissner, N. S. Sariciftci, I. Riedel, V. Dyakonov, and J. Parisi, Appl. Phys. A **79**, 1 (2004).
[3] S. Pfuetzner, J. Meiss, A. Petrich, M. Riede, and K. Leo, Appl. Phys. Lett. **94**, 253303 (2009).
[4] M. Riede, T. Mueller, W. Tress, R. Schueppel, and K. Leo, Nanotechnology **19**, 424001 (2008).
[5] S. M. Sze, *Physics of Semiconductor Devices*, 2nd ed. (Wiley-Interscience, New York, 1981).
[6] V. D. Mihailetchi, J. Wildeman, and P. W. M. Blom, Phys. Rev. Lett. **94**, 126602 (2005).
[7] D. Ray, M. P. Patankar, G. H. Dohler, and K. L. Narasimhan, J. Appl. Phys. **100**, 113727 (2006).
[8] D. Ray, M. P. Patankar, N. Periasamy, and K. L. Narasimhan, J. Appl. Phys. **98**, 123704 (2005).
[9] L. J. A. Koster, E. C. P. Smits, V. D. Mihailetchi, and P. W. M. Blom, Phys. Rev. B **72**, 085205 (2005).
[10] C. Waldauf, M. C. Scharber, P. Schilinsky, J. A. Hauch, and C. J. Brabec, J. Appl. Phys. **99**, 104503 (2006).
[11] R. S. Crandall, J. Appl. Phys. **53**, 3350 (1982).
[12] P. Schilinsky, C. Waldauf, J. Hauch, and C. J. Brabec, J. Appl. Phys. **95**, 2816 (2004).
[13] R. S. Crandall, J. Appl. Phys. **54**, 7176 (1983).
[14] S. Barth and H. Bassler, Phys. Rev. Lett. **79**, 4445 (1997).
[15] M. Pope and C. E. Swenberg, *Electronic Processes in Organic Crystals and Polymers*, 2nd ed. (Oxford University Press, New York, 1999).
[16] L. Onsager, Phys. Rev. **54**, 554 (1938).
[17] R. H. Batt, C. L. Braun, and J. F. Hornig, J. Chem. Phys. **49**, 1967 (1968).
[18] R. R. Chance and C. L. Braun, J. Chem. Phys. **59**, 2269 (1973).
[19] R. R. Chance and C. L. Braun, J. Chem. Phys. **64**, 3573 (1976).
[20] P. M. Borsenberger, J. Chem. Phys. **69**, 5210 (1978).
[21] C. L. Braun, J. Chem. Phys. **80**, 4157 (1984).
[22] Z. D. Popovic, Chem. Phys. **86**, 311 (1984).
[23] P. J. Bounds and W. Siebrand, Chem. Phys. Lett. **75**, 414 (1980).
[24] L. Sebastian, G. Weiser, G. Peter, and H. Bassler, Chem. Phys. **75**, 103 (1983).
[25] L. Luer, C. Manzoni, H.-J. Egelhaaf, G. Cerullo, D. Oelkrug, and G. Lanzani, Phys. Rev. B **73**, 035216 (2006).
[26] S. Barth, H. Bassler, H. Rost, and H. H. Horhold, Phys. Rev. B **56**, 3844 (1997).
[27] S. Barth, H. Bassler, T. Wehrmeister, and K. Mullen, J. Chem. Phys. **106**, 321 (1997).
[28] A. K. Ghosh and T. Feng, J. Appl. Phys. **49**, 5982 (1978).
[29] V. Bulovic and S. R. Forrest, Chem. Phys. **210**, 13 (1996).
[30] V. Bulovic and S. R. Forrest, Chem. Phys. Lett. **238**, 88 (1995).
[31] D. E. Markov and P. W. M. Blom, Phys. Rev. B **72**, 161401(R) (2005).
[32] D. E. Markov, C. Tanase, P. W. M. Blom, and J. Wildeman, Phys. Rev. B **72**, 045217 (2005).
[33] A. A. Zanfolim, D. Volpati, C. A. Olivati, A. E. Job, and C. J. L. Constantino, J. Phys. Chem. C **114**, 12290 (2010).
[34] M. Wojdyla, B. Derkowska, Z. Lukasiak, and W. Bala, Mater. Lett. **60**, 3441 (2006).
[35] S. Senthilarasu and S. H. Lee, Cryst. Res. Technol. **42**, 504 (2007).
[36] B. Maennig, M. Pfeiffer, A. Nollau, X. Zhou, K. Leo, and P. Simon, Phys. Rev. B **64**, 195208 (2001).

[37]R. Schmechel, J. Appl. Phys. **93**, 4653 (2003).
[38]D. Ray, L. Burtone, K. Leo, and M. Riede, Phys. Rev. B **82**, 125204 (2010).
[39]A. M. Saleh, A. K. Hassan, and R. D. Gould, J. Phys. Chem. Solids **64**, 1297 (2003).
[40]I. Kim, H. M. Haverinen, Z. Wang, S. Madakuni, Y. Kim, J. Li, and G. E. Jabbour, Chem. Mater. **21**, 4256 (2009).
[41]Y. Terao, H. Sasabe, and C. Adachi, Appl. Phys. Lett. **90**, 103515 (2007).
[42]R. Schueppel, R. Timmreck, N. Allinger, T. Mueller, M. Furno, C. Uhrich, K. Leo, and M. Riede, J. Appl. Phys. **107**, 044503 (2010).
[43]L. A. A. Pettersson, L. S. Roman, and O. Inganas, J. Appl. Phys. **86**, 487 (1999).
[44]J. Meiss, M. Furno, S. Pfuetzner, K. Leo, and M. Riede, J. Appl. Phys. **107**, 053117 (2010).
[45]E. Centurioni, Appl. Opt. **44**, 7532 (2005).
[46]R. Seoudi, G. S. El-Bahy, and Z. A. El Sayed, Opt. Mater. **29**, 304 (2006).
[47]G. S. S. Saini, S. Singh, S. Kaur, R. Kumar, V. Sathe, and S. K. Tripathi, J. Phys. Condens. Matter **21**, 225006 (2009).
[48]A. Ogunsipe, D. Maree, and T. Nyokong, J. Mol. Struct. **650**, 131 (2003).
[49]A. M. Goodman and A. Rose, J. Appl. Phys. **42**, 2823 (1971).
[50]R. S. Crandall, in *Semiconductors and Semimetals*, Hydrogenated Amorphous Silicon, Part B, Optical Properties, edited by J. I. Pankove, Vol. 21 (Academic Press, Orlando, FL, 1984), pp. 245–297.
[51]H. Bassler, Phys. Status Solidi (B) **175**, 15 (1993).
[52]P. M. Borsenberger, L. Pautmeier, and H. Bassler, J. Chem. Phys. **94**, 5447 (1991).
[53]W. Brutting, S. Berleb, and A. G. Muckl, Organic Electronics **2**, 1 (2001).
[54]P. B. Miranda, D. Moses, and A. J. Heeger, Phys. Rev. B **64**, 081201 (2001).
[55]A. Kohler, D. A. dos Santos, D. Beljonne, Z. Shuai, J.-L. Bredas, A. B. Holmes, A. Kraus, K. Mullen, and R. H. Friend, Nature **392**, 903 (1998).
[56]C. Silva, M. A. Stevens, D. M. Russell, S. Setayesh, K. Mullen, and R. H. Friend, Synth. Met. **116**, 9 (2001).
[57]C. Schunemann, C. Elschner, A. A. Levin, M. Levichkova, K. Leo, and M. Riede, Thin Solid Films **519**, 3939 (2011).
[58]J. J. Kwiatkowski, J. M. Frost, and J. Nelson, Nano Lett. **9**, 1085 (2009).